Modeling Disinhibition within a Layered Structure of the LGMD neuron

Ana Silva and Cristina P Santos

***Abstract*—Due to their relatively simple nervous system, insects are an excellent way through which we can investigate how visual information is acquired and processed in order to trigger specific behaviours, as flight stabilization, flying speed adaptation, collision avoidance responses, among others. From the behaviours previously mentioned, we are particularly interested in visually evoked collision avoidance responses. These behaviors are, by necessity, fast and robust, making them excellent systems to study the neural basis of behavior. On the other hand, artificial collision avoidance is a complex task, in which the algorithms used need to be fast to process the captured data and then perform real time decisions. Consequently, neurorobotic models may provide a foundation for the development of more effective and autonomous devices.**

In this paper, we will focus our attention in the Lobula Giant Movement Detector (LGMD), which is a visual neuron, located in the third layer of the locust optic lobe, that responds selectively to approaching objects, being responsible for trigger collision avoidance maneuvers in locusts. This selectivity of the LGMD neuron to approaching objects seems to result from the dynamics of the network pre-synaptic to this neuron. Tipically, this modelation is done by a conventional Difference of Gaussians (DoG) filter. In this paper, we propose the integration of a different model, an Inversed Difference of Gaussians (IDoG) filter, which preserves the different level of brightness in the captured image, enhancing the contrast at the edges. This change is expected to increase the performance of the LGMD model. Finally, a comparative analysis of both modelations, as well as its effect in the final response of the LGMD neuron, will be performed.

I. Introduction

Visual neurons that respond selectively to approaching objects have been studied across very different animal species, as humans, monkeys, pigeons, turtles, flies, locusts, among others[1]. From the animals previously mentioned, insects, as flies and locusts, are particularly interesting from an engineer point-of-view: many insects are able to perform, fast and robustly, different behaviours, despite their low-resolution vision and limited neural resources [2]. Due to these reasons, they became rich sources of inspiration to engineers seeking to emulate insect-level performance with low computational resources[3].

Ana Silva and Cristina P Santos are with the Department of Industrial Electronics, at University of Minho, Portugal. (Email: {ana.silva, cristina}@dei.uminho.pt)

Ana Silva is supported by PhD Grant SFRH/BD/70396/2010. This work is funded by FEDER Funds through the Operational Programme Competitiveness Factors - COMPETE and National Funds through FCT - Foundation for Science and Technology under the Project: FCOMP-01-FEDER-0124-022674.

Unlike vertebrates, insects have immobile eye with fixed-focus optics. Due to this reason, they can not infer the distance of an object from the extent to which the directions of gaze must converge to see the object, neither by monitoring the refractive power needed to bring the object's image into focus on the retina [4]. Consequently, insects have evolved alternative visual strategies to drive their behaviour in the three-dimensional world: insects usually use cues extracted from the image motion experienced as they move in the environment[5]. For example, image expansion, which is a visual cue generated by an approaching object, is used by insects to avoid imminent collisions [6], [7]. So, certain neural mechanisms in insect visual system must be tuned to detect image expansion.

One of these neural mechanisms, part of the locust visual system, is the Lobula Giant Movement Detector (LGMD) neuron. This neuron generates a vigorous and prolonged train of spikes in response to an approaching object [8], [9], [10]. However, images of receding or translating objects generate only brief responses. According to literature[11], this preference of the LGMD neuron to approaching objects could result from the dynamics of the its pre-synaptic network. In consequence to this previous consideration, two inevitable reserach questions arise:

How is the LGMD pre-synaptic network able to compute image expansion?

Does different modelation of early vision processing affect the final response of the LGMD neuron?

According to literature, the first physiological and anatomical LGMD model was developed by Bramwell in [12]. The model continued to evolve [13], [14], [15], [16] and it was used in mobile robots and deployed in automobiles for collision detection. However, to the best of our knowledge, no attention was given on the effect that different modelations of early stages of visual processing in the locust optic lobe have in the final response of the LGMD model.

In this paper we propose the implementation of two different filters to model the first stage of visual processing in the locust optic lobe: a Difference of Gaussians filter (DoG), used previously within a LGMD model [11]; and an innovative approach, using an Inverted Difference of Gaussians filter (IDoG) [17]. This innovative approach introduces disinhibition within our model, leading to a preservation of the different level of brightness in the captured image, as well as to an enhancement in the contrast at the edges.

The proposed integration of disinhibion in our model increases the overlap between the model output and the biological results to the same visual stimuli. When stimulated with images containing a high noise level, the LGMD model with IDoG filter proved to be very robust at the object

approaching detection. Besides that, when tested in a real environment, the results were also very satisfactory.

To a better understanding of the work here presented, the paper was organized in the following way. In section II, we make a first short description of the locust visual neurons, which are integrated in the neural network responsible for trigerring collision avoidance behaviours. In section III, we make a detailed description of the proposed LGMD model. In section IV are presented some experimental results on simulated and recorded video data. Finally, in section V, we discuss the conclusions of the work here described.

II. Visual information processing

At insect level, the interneurons that process visual information are arranged in a serie of neuropiles, distributed beneath the compound eye, making up the optic lobe [18]. The visual information flows within and through different layers in the optic lobe, either sequentially or laterally (by lateral connections).

The first processing in the locust visual system is done by photoreceptors, which convey a representation of the environment[19] to the first neuropile, Lamina. Based on [20], [21], the role of early sensory processing, performed by neurons located in the lamina, is to reduce redundancy and recode the sensory input into an efficient form. This should be done because natural signals are highly redundant, due to the tendency towards spatial and temporal uniformity of these signals[22]. So, a neural direct representation of the raw image would be inefficient. An important way to achieve this goal is to perform predictive coding. According to this approach, neural networks learn the statistical distributions inherent in images and reduce redudancy by removing the predictable components of the input, transmitting just what is not predictable [23]. This is a possible explanation to the centre-surround antagonism in the receptive fields of visual interneurons found in very different animals species [20]. The antagonistic surround takes a weighted mean of the signal in the neighbouring receptors to generate a statistical prediction of the signal at the centre. Then, the predicted value is subtracted from the actual centre signal, minimizing the range of outputs transmitted. This process decorrelates the input signals by flattening the spatial and temporal power spectra, leading to a reduction of the output redudancy[21]. This kind of inhibition in sensory system is known as lateral inhibition. Difference of Gaussians (DoG) filter is usually used to simulate such process [11].

However, anatomical and physiological experiments have shown that this centre-surround property may not be strictly feed-forward: the process involves a recurrent inhibition, which leads to disinhibition [24]. Hartline *et al.* [24]used the Limulus optical cells to demonstrate the lateral inhibition and disinhibition effects in the receptive fields of the Limulus visual system. In this paper, it was demonstrated that disinhibition is able to reduce the amount of inhibition in the presence of a large area of light input. Based on these biological considerations, Yue and Choe [17] proposed a new filter that is able to incorporate the disinhibitory effect. They named it as an Inverted Difference of Gaussian filter (named IDoG filter). However, this filter had not yet been attempted in a LGMD model to achieve collision avoidance. In section III, we will describe in detail the mathematical formulation of the IDoG filter.

Based on these two modelations of spatial predictive coding, we decided to implement both to model the visual processing at the Lamina level, and analyze the effect that this different modelation has in the final response of the LGMD model.

Beyond space domain, predictive coding can also be applied in time: the current intensity can be predicted as a weighted linear combination of intensities past history [23]. Based on this principle, we modeled the second layer of the optic lobe, named Medulla, as a temporal filter that highlights changes in intensity across time.

At last, the neuron responsible for triggering collision avoidance reactions in locusts, the LGMD neuron, located in the third layer of the locust optic lobe, the Lobula, integrates the output of the neurons from the medulla layer [25].

Taking into account the previous considerations, we propose a new LGMD model, which integrates predictive coding, either in spatial and temporal domain. We will make a comparative analysis between the traditional modelation of the Lamina neurons (through a DoG filter) and the IDoG filter proposed in [17], as well as the effect of these different modelations in the final response of the LGMD neuron.

III. Model

The model here proposed is insect based and, consequently, it models several processes performed in different layers of the insect visual system. It is composed by three different groups of neurons: Photoreceptor neurons (P layer), Lamina neurons (L layer), Medulla neurons (M layer); and by one single neuron: the LGMD neuron (see figure 1).

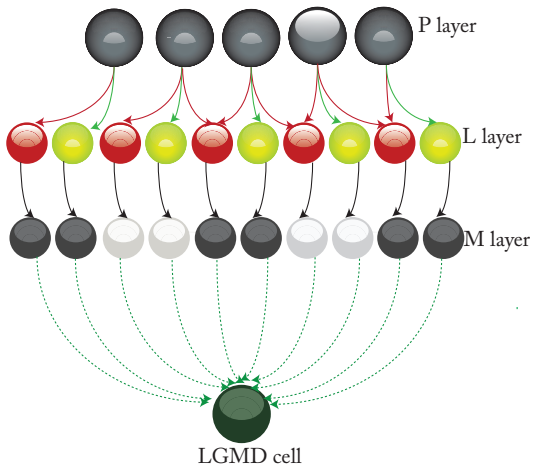

Figure 1. Schematic illustration of the proposed LGMD model.

A. Photoreceptive layer

A grayscale image of the camera current field of view, represented has a matrix of values (from 0 to 255), is the input to a matrix of photoreceptor units (P layer). The output of the P layer is the input of the next layer, the Lamina.

$$P_f(x, y) = I_f(x, y) \tag{1}$$

$P_f(x, y)$ is the output from the Photoreceptor cell at position (x, y) for frame f and $I_f(x, y)$ is the intensity of the the pixel, captured by the camera, at position (x, y) for frame *f*.

B. Lamina layer

Lamina cells receive the output of the photoreceptive cells and, as previously mentioned, model the spatial predictive coding strategy. In this paper, we will model the spatial predictive coding through two different strategies:

1. Difference of Gaussians (DoG) filter: the central receptors produce an excitatory signal, while cells in the surrounding area send inhibition through lateral connections to the central area.

2. Inverted Difference of Gaussians (IDoG) filter: based on the principle that centre-surround property in early visual processing may not be strictly feed-forward, involving lateral inhibition and, moreover, disinhibition.

In IDoG filter, the response of *n* cells can be expressed in matrix form as:

$$W \times l_f = p_f \tag{2}$$

l is the output vector, *p* is the input vector (pixel intensity), both for frame *f*, and *W* is the weight matrix:

$$l_f = \begin{bmatrix} l_1 \\ l_2 \\ ... \\ l_n \end{bmatrix}, \; p_f = \begin{bmatrix} p_1 \\ p_2 \\ ... \\ p_n \end{bmatrix}, \quad W = \begin{bmatrix} 1 & -w(1) & ... & -w(n-1) \\ -w(1) & 1 & ... & -w(n-2) \\ ... & ... & ... & ... \\ -w(n-1) & ... & ... & 1 \end{bmatrix} \tag{3}$$

In order to get the value of W_{ij} from neuron *j* to neuron *i*, a classical two-mechanism DoG distribution is applied:

$$W(i,j) = \begin{cases} -w(|i,j|) \; when \; i \neq j \\ 1 \; when \; i = j \end{cases} \tag{4}$$

$$w(d) = DoG(d) = k_c e^{(-d/\sigma_c)^2} - k_s e^{(-d/\sigma_s)^2} \tag{5}$$

where $|i, j|$ is the Euclidian Distance (d) between neuron i and j; k_c and k_s are the scaling constants that determine the relative scale of the excitatory and inhibitory distributions, and σ_c and σ_s their widths[17].

The response vector (l) can be derived from equation 2 as:

$$l_f = W^{-1} \times p_f \tag{6}$$

One limitation of this approach is that the inversed weight matrix results in a non-local operation, which could lead to an inefficient computation. In order to overcome this problem, we use an approximated algorithm, through which we can use a local convolution operation to process our images[17].

Consequently, the output from each neuron in the Lamina (L) layer is given by:

$$L_f(x, y) = \sum_{i=-4}^{4} \sum_{j=-4}^{4} P_f(x + i, y + j) \cdot F(i, j), \tag{7}$$

where $L_f(x, y)$ is the Lamina cell value at position (x, y) for frame f; $P_f(x, y)$ is the output from the Photoreceptor cell at position (x, y) for frame *f; F* is the filter used in the convolution process, which can be a DoG or an IDoG filter.

In both filters, the parameters used for both filters are listed in table I. In all the experiments done, the weight of excitatory and inhibitory contributions should be kept the same, because following the principles of predictive coding, the excitation and inhibition should cancell each other and, consequently, their weights should be the same.

Table I. PARAMETER VALUES OF THE LAMINA MODEL.

Parameter	Value
Filter size	9×9
σ_c	$\frac{\text{Filter size}}{20}$
σ_s	$\frac{\text{Filter size}}{6}$
$k_c = k_s$	1.0

C. Medulla Layer

In the Medulla level, each neuron computes the actual intensity level through a temporal prediction, modeled as a weighted linear combination of the past history of intensity in each pixel. So, for each frame *f,* the value of each Medulla neuron is given by:

$$M_f(x, y) = \sum_{i=0}^{f-j} h_i . L_{f-i}(x, y) \tag{8}$$

where f indicates the current sample and the set of temporal coefficients (showed on figure 2) is $\{h_i : i = 0, 1, f-j\}$, being $(f-j+1)$ the number of samples included in the filter. $\{L_i : i = j, j+1, ..., f\}$ are the values of Lamina neurons during the last $(f - j + 1)$ frames, and L_f is the most recent.

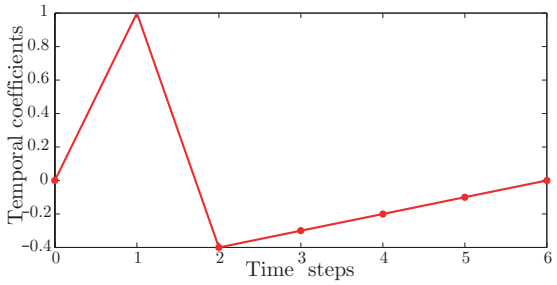

Figure 2. Temporal coefficients used in the modelation of the Medulla layer.

D. LGMD neuron

In this paper, the LGMD neuron makes the simple integration from all cells located in the previous layer, the Medulla, being mathematically represented by:

$$\mathrm{LGMD}_f = \frac{|\sum_{x=1}^{n}\sum_{y=1}^{m} M_f(x,y)|}{n \cdot m}, \qquad (9)$$

where *n* is the number of rows and *m* is the number of columns of the matrix representing the captured image.

IV. Experimental results: comparative analysis

In a way to test the efficiency of the LGMD model proposed, two experimental scenarios were used. The first experiment was made on a simulated data set and, in the second, we used a recorded video to prove the capability of the LGMD model to deal with a real environment.

A. Simulated environment

We developed a simulation environment in Matlab, which enables us to assess the effectiveness of the proposed model. Objects were simulated according to their movement and the corresponding data was acquired by a simulated camera and processed by the model. Image sequences were generated by a simulated camera with a field of view of 60º in both x and y axis, a sampling frequency of 100 Hz, and a resolution of 100 by 100 pixels.

The simulated environment enables us to adjust several parameters, such as: image matrix dimensions, camera rate of acquisition, image noise level, object shape and texture, among other parameters. The computer used was a Laptop (Toshiba Portegé R830-10R) with 4 GHz CPUs and Windows 7 operating system.

B. Spatial decorrelation of the input signals through a DoG and IDoG filter

As previously mentioned, both DoG and IDoG filters, here modeling the neural processing done by the neurons in the Lamina layer, have a specific function within the network: reduce redundancy and recode the sensory input into an efficient form. This process will decorrelate the input signal. The minimum possible autocorrelation for a given signal energy is achieved by equalising the power spectra of the signal to be similar to that of a white noise signal, which is a random signal with a flat/constant power spectral density. Consequently, the lower is the slope of the spatial power spectrum obtained, more the output redundancy is reduced.

In order to verify which filter decorrelates the input signal in a more efficient way, *i.e.*, the one which leads to a higher flattening of the spatial power spectra slope, without changing the power spectrum (the power spectra should keep its shape under such process, changing only the slope), we perform a comparative analysis of the power spectra relative to the original frame (composed by a black square over a white background), as well the result obtained from the DoG and IDoG filter applied to the original frame, respectively.

Observing figure 3, we observe that, when we applied a IDoG filter, the slope of the relation between the power and the frequency components of the image was flatenned and the variations within the power spectrum kept almost equal

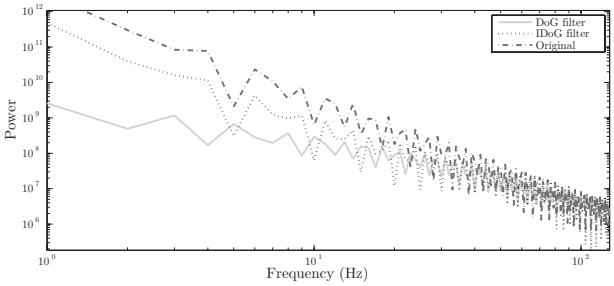

Figure 3. Power spectrum of an original frame (black square over a white background, slope equal to -2.87), as well as the frame output of the Lamina layer when using an IDoG (slope equal to -2.26) and a DoG(slope equal to -1.54) spatial filters, averaged over all orientations.

to the original frame. In relation to the application of the DoG filter, we verify that the application of this filter has a higher effect on the flatenning process, but it highly changes the variations of the power spectra when compared with the original frame.

In order to analyse the effect that different excitatory/inhibitory receptive field contributions have on the power spectrum obtained, the inhibitory contribution used by the DoG filter, defined by the parameter k_s in equation 5, was progressively decreased in steps of 0.1. The different power spectra obtained for each k_s value showed that the application of the IDoG filter was always more effective in reducing the redundancy of the input signal because it flattens the slope, keeping, at the same time, the variations within the power spectra (see figure 3).

C. Model validation

Validation is a necessary step for model acceptance. In a first step, we analysed the response of the LGMD model here proposed, using, in the lamina layer, both DoG and IDoG filters, to a set of standard LGMD stimulation protocols. This process allowed us to validate our model with respect to the biological system. Firstly, we evaluated the LGMD model, by using a looming stimulus consisting of a solid square with 10 repetitions to each size/velocity = $l/|v|$ pair (where l stands for the half length of the square object and v for its linear velocity). With these experiments, we wanted to verify that our model respects the properties verified in biology, as well as in models previously proposed in literature [7], [11]. These properties, founded in the locust visual system, include a linear relation between the time of the peak firing rate of the LGMD neuron and the ratio that correlates the stimulus object size (l) and the stimulus linear velocity (v) [25], as well as a near-exponential decay in the peak firing rate as the $l/|v|$ ratio increases.

Taking into account the previous considerations, we analysed the proposed LGMD model using a black square looming stimulus. This procedure was repeated to a range of ten different $l/|v|$ ratios. During this process of validation, our first step was to verify if the relation between the time of the peak firing rate, produced by our model(top panel on figure 4), and the $l/|v|$ ratio of the approaching visual stimuli, was linear.

Through the obtained results we conclude that the fit of the TTC (time-to-collision) of the peak firing rate, for both

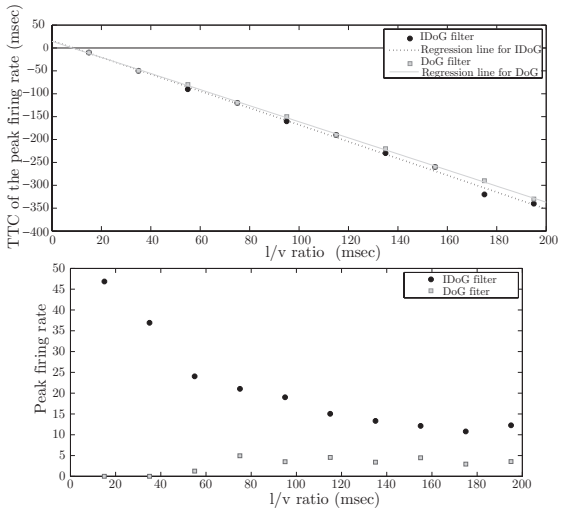

Figure 4. Top: Dependence of peak firing time relative to collision on *l*/|*v*| ratio obtained with the LGMD model, using a DoG filter as a model for the Lamina processing step (gray squares) and using a IDoG filter (black dots). Bottom: Relation between the peak firing rate obtained in the output of the LGMD cell and the *l*/|*v*| ratio.

DoG and IDoG filters, is consistent with the biological results (figure 4, top), showing a correlation coefficient (r) near to 0.99.

In the second step of the validation process, we expected to observe a near-exponential decay in the peak firing rate in relation to the increment of the *l*/|*v*| ratio.

Although no significant differences were found in the linear regression lines that relate the TTC of the peak firing rate and *l*/|*v*| ratios for the different modelations of Lamina processing method, considerable differences were found in the relation of the peak firing rate and the *l*/|*v*| ratios when an IDoG or a DoG filter was implemented (bottom panel in figure 4). Only when a IDoG filter was used to model the Lamina processing mechanism, the obtained results were consistent with the biological ones: in bottom panel of 4, the black dots amplitude decreases near-exponentially as the ratio *l*/|*v*| increases. The implementation of the DoG filter kept the peak of the LGMD firing rate constant at very low levels of spike rate at a high range of different *l*/|*v*| ratios.

If, in biology, the LGMD neuron is responsible for triggering escape responses, the spike rate profile of this neuron should be encoded independently of the particular properties of the looming stimuli. In order to verify if this hypothesis, *i.e.*, the invariant properties of the LGMD response to the shape, texture and approaching angle of the visual stimulus, is observed in the model here proposed, a serie of experiments were done. For that, four different stimuli were developed in Matlab: the first is the one previously described, a single black square, with a white background, approaching at different $l/|v|$ ratios. The second stimulus developed is a black circle, with a white background, approaching also at different $l/|v|$ ratios. The third visual stimulus is a square with a checkerboard texture. Finally, the last visual stimulus is a simple square deviated 50 degrees relatively to the center of the camera that generates the visual stimuli.

Even though the total amount of the spikes produced by the LGMD model was reduced for the case of a misalignment of 50 degrees, resulting from the loss of stimulation by the looming stimulus (as the object approaches, part of the visual stimuli remains outside the screen), we verified that the linear relation between the TTC of peak firing rate and the *l*/|*v*| ratio was not affected by all the different characteristics of visual stimuli ($r \approx 0.98$).

According to the obtained results previously described, we conclude that the intrinsic linear dependence between the peak firing time and the *l*/|*v*| ratio remains preserved by the LGMD model here proposed.

D. Results: simulated data set

Despite the better results, previously described in the validation process, when using the IDoG filter, comparatively to the DoG filter, we have decided to implement both filters as the modelation of Lamina layer, in order to compare the obtained results.

In this step, we fed the LGMD model proposed in this article, with simulated image sequences, with different signal to noise ratios (a representation can be observed on figure 5). Four different simulated visual stimuli of a black approaching square, over a white background, with l/|v| equal to 50 milliseconds, acquired with a frame rate of 100 Hz, were produced to verify our aims. Stimuli differ on the noise level: Simulus 1: no noise was added to the image sequence. Stimulus 2: has a Signal-to-Noise ratio equal to 9. Stimulus 3: has a Signal-to-Noise ratio equal to 2.33. Stimulus 4: has a Signal-to- Noise ratio equal to 1.0.

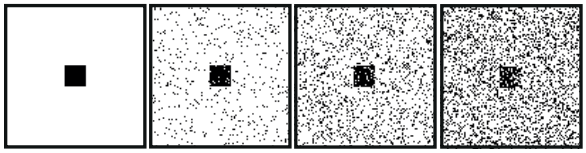

Figure 5. Selected frames from the simulated image sequence, for different noise levels. From left no right: Signal to noise-ratio (S/N)=∞; S/N=9; S/N=2.33; S/N=1.0.

The obtained results can be seen in figure 6.

Observing the spike rate profile of the LGMD model here proposed, when implementing the IDoG filter (top panel on figure 6) and comparing it to the biological LGMD neuron spike rate described in literature [7], [6], [26], [27], we conclude that they are quite similar, even for very low signal-to-noise ratios (stimulus 3 and 4). Even when using Stimulus 4, the ratio between the peak spike rate (at t=-0.08 seconds) and the highest value of spike rate produced by noise (at t=-0.48 seconds) is 12. However, for the same situation tested, but replacing the IDoG by a DoG filter (middle panel on figure 6), the firing rate profile is no longer similar to the biological one.

Besides that, when using stimulus 4, the ratio between the peak spike rate (at t=-0.08 seconds) and the highest value of spike rate produced by noise (at t=-0.46 seconds) decreases to 3.4. Through this difference, we verify the robustness added to the model when a IDoG filter is used, comparatively to the modelation done by a DoG filter.

By applying a simple threshold mechanism to the output of this model using the IDoG filter, we could easily create a collision avoidance artificial mechanism.

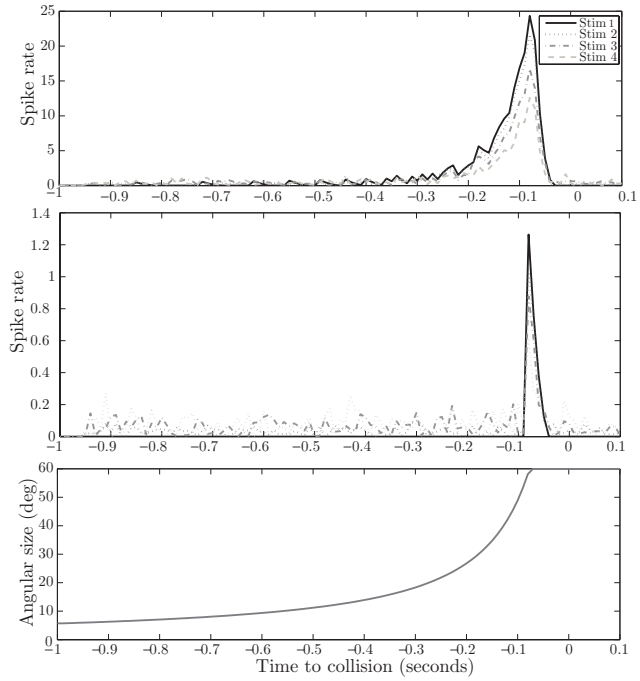

Figure 6. Top panel: LGMD model response to an approaching object with $l/|v|$ set at 50 milliseconds, with four different signal-to-noise ratios for IDoG filter. Middle panel: LGMD model response to an approaching object with $l/|v|$ set at 50 milliseconds, with four different signal-to-noise ratios for DoG filter. Bottom panel: angular size of the approaching object.

E. Results: Real recorded data

In order to test the capability of the proposed LGMD model to work in a realistic environment, we subjected it to a real video sequence showing an approaching ball, with $l/|v| \simeq 30$ ms (see figure 7). A PlayStation Eye digital camera was used to obtain the video clip. The resolution of the video images was 640×480 pixels, with an acquisition frequency of 70 frames per second. The background of the real image sequence is composed by multiple and different static objects.

Despite the complexity of the environment (see figure 7), the LGMD model has produced the expected spike rate, which peak ocurred before the predicted time of collision (indicated by a red line in figure 7)

These results indicate that this model could easily be deployed as a collision detector in robotic applications.

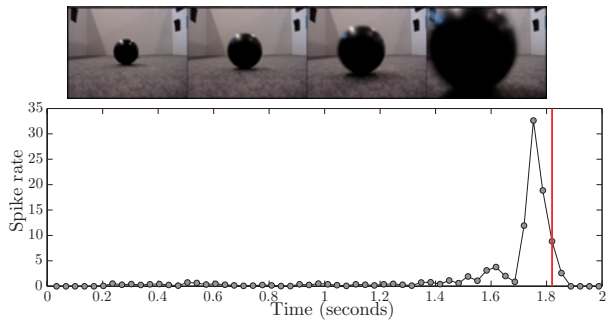

Figure 7. Selected frames from the recorded image sequence used in the experiment and the respective spike rate obtained (red vertical line indicates the time of collision).

V. Conclusions

In this paper, we propose a different model of the LGMD neuron, introducing concepts of spatial and temporal predictive coding. In order to achieve spatial redudancy reduction, we proposed two spatial filters: the DoG and IDoG filter. A recent published research[11], discussed that the non-linearity of the LGMD neural responses results as an emergent property of affererent networks. We base ourselves on these findings, and decided to analyze the difference between the application of an DoG and IDoG filter and the effect that it has on the final response of the LGMD model. After a deep validation, we observed that, when we implement a DoG filter, the final response of the LGMD model was quite different from the biologic responses. However, the implementation of the IDoG filter led to a very similar response of both artificial and real LGMD neurons.

After the model validation, using artificial and real image sequences, we showed the capability of the model to continue producing good results even in very low signal-to-noise ratios. This property endow, to our model, a very high robustness to complex environments.

As future work, we propose to continue enhancing this approach, using, for that, a combination of physiological and anatomical studies of the locust visual system, in order to improve our undertanding about the relation between the LGMD neuron output and the locust muscles related to avoidance manoeuvres.

References

[1] Haleh Fotowat and Fabrizio Gabbiani. Collision Detection as a Model for Sensory-Motor Integration. *Annual review of neuroscience*, 34:1–19, July 2010.

[2] N. Franceschini, J. M. Pichon, and C. Blanes. From insect vision to robot vision. *Phil. Transactions on R. Soc. Lond. A*, 337:283–294, 1992.

[3] Haiyan Wu, Ke Zou, Tianguang Zhang, Alexander Borst, and Kolja Kühnlenz. Insect-inspired high-speed motion vision system for robot control. *Biological Cybernetics*, 106(8):453–463, October 2012.

[4] Mandyam V Srinivasan and Shaowu Zhang. Visual motor computations in insects. *Annu Rev Neurosci*, 27:679–96, 2004.

[5] A. Borst and M. Egelhaaf. Detecting visual motion: theory and models. In Wallman J Miles FA, editor, *Visual motion and its role in the stabilization of gaze*, pages 3–27. Elsevier, New York, 1961.

[6] John R Gray, Jessica K. Lee, and R. Meldrum Robertson. Activity of descending contralateral movement detector neurons and collision avoidance behaviour in response to head-on visual stimuli in locusts. *Journal of Comparative Physiology A*, 187:115–129, March 2001.

[7] Fabrizio Gabbiani, Holger G. Krapp, and Gilles Laurent. Computation of object approach by a wide-field motion-sensitive neuron. *The Journal of Neuroscience*, 19:1122–1141, 1999.

[8] F. C. Rind and P. J. Simmons. Signaling of object approach by the DCMD neuron of the locust. *Journal of neurophysiology*, 77(2):1029–1033, February 1997.

[9] F. Gabbiani, C. Mo, and G. Laurent. Invariance of angular threshold computation in a wide-field looming-sensitive neuron. *The Journal of neuroscience : the official journal of the Society for Neuroscience*, 21:314–329, 2001.

[10] G.A. McMillan and J.R. Gray. Responses of a motion sensitive neuron to changes in object trajectory. *Proceedings of the 7th International Congress of Neuroethology*, 2007.

[11] Sergi Bermudez i Badia, Ulysses Bernardet, and Paul F. M. J. Verschure. Non-linear neuronal responses as an emergent property of afferent networks: A case study of the locust lobula giant movement detector. *PLoS Comput Biol*, 6(3):e1000701, March 2010.

[12] Rind and D. I. Bramwell. Neural network based on input organization of an identified neuron signaling impending collision. *Jour. Neurophysiol.*, 75:967–985, 1996.

[13] J. Silva A. Silva and C. P. Santos. Lgmd based neural network for automatic collision detection. In *Proceedings of the 9th International Conference on Informatics in Control, Automation and Robotics, Rome, Italy*, 2012.

[14] Blanchard M., Rind F.C., and Verschure P.F.M.J. Collision avoidance using a model of the locust lgmd neuron. *Robotics and Autonomous Systems, 2010*, 30.

[15] Shigang Yue and F. Claire Rind. Collision detection in complex dynamic scenes using an lgmd-based visual neural network with feature enhancement. *IEEE Transactions on Neural Networks, 2006*.

[16] Hongying Meng, Kofi Appiah, Shigang Yue, Andrew Hunter, Mervyn Hobden, Nigel Priestley, Peter Hobden, and Cy Pettit. A modified model for the lobula giant movement detector and its fpga implementation. *Computer Vision and Image Understanding*, 114(11):1238 – 1247, 2010.

[17] Yingwei Yu and Yoonsuck Choe. A neural model of the scintillating grid illusion: Disinhibition and self-inhibition in early vision. *Neural Computation*, 18(3):521–544, 2006.

[18] P.J. Simmons and D. Young. *Nerve Cells and Animal Behaviour*. Cambridge University Press, 2010.

[19] M Wilson, P Garrard, and S McGinness. The unit structure of the locust compound eye. *Cell Tissue Res*, 195(2):205–26, 1978.

[20] M. V. Srinivasan, S. B. Laughlin, and A. Dubs. Predictive coding: a fresh view of inhibition in the retina. *Proceedings of the Royal Society of London. Series B, Containing papers of a Biological character. Royal Society (Great Britain)*, 216(1205):427–459, November 1982.

[21] Yanping Huang and Rajesh P. N. Rao. Predictive coding. *WIREs Cogn Sci*, 2(5):580–593, 2011.

[22] Toshihiko Hosoya, Stephen A. Baccus, and Markus Meister. Dynamic predictive coding by the retina. *Nature*, 436(7047):71–77, July 2005.

[23] E. P. Simoncelli and B. A. Olshausen. Natural image statistics and neural representation. *Annual Review of Neuroscience*, 24:1193–1216, 2001.

[24] H. K. Hartline and Floyd Ratliff. Inhibitory interaction of receptor units in the eye of limulus. *The Journal of General Physiology*, 40(3):357–376, January 1957.

[25] Fabrizio Gabbiani, Holger G. Krapp, Christof Koch, and Gilles Laurent. Multiplicative computation in a visual neuron sensitive to looming. *Nature*, 420:320–324, November 2002.

[26] John Gray, Eric Blincow, and R. Robertson. A pair of motion-sensitive neurons in the locust encode approaches of a looming object. *Journal of Comparative Physiology A: Neuroethology, Sensory, Neural, and Behavioral Physiology*, 196:927–938, 2010. 10.1007/s00359-010-0576-7.

[27] F. C. Rind and P. J. Simmons. Local circuit for the computation of object approach by an identified visual neuron in the locust. *Journal of Comparative Neurology*, 395:405–415, 1998.